ELSEVIER

Coastal Engineering 42 (2001) 241–256

Coastal Engineering
An International Journal for Coastal, Harbour and Offshore Engineers

www.elsevier.com/locate/coastaleng

The pressure impulse in a fluid saturated crack in a sea wall

Simon J. Cox *, Mark J. Cooker

School of Mathematics, University of East Anglia, Norwich, NR4 7TJ, UK

Received 2 July 1999; received in revised form 31 July 2000; accepted 27 September 2000

Abstract

When a wave breaks against a sea wall containing a crack, such as might exist within the blockwork, pressure pulses can travel through the fluid and propagate into the crack. This can cause high stresses to act on the sides and roof of the crack and may even cause the constituent blocks to move. The Pressure Impulse, P, is used to model the effect of wave impact against a wall in which there is a fluid filled crack. A two-dimensional field equation is derived for P that is applicable in plane cracks of non-uniform, narrow width. This is solved for several geometries relating to cracks between constituent blocks of sea walls, in order to compare the impulsive forces with the gravitational force on a block. It is shown that a large block can be lifted due to the impulse exerted by the fluid in a crack beneath it.

Keywords: Breaking waves; Breakwaters; Cracks; Impacts; Pressure impulse

1. Introduction

This paper presents a theoretical investigation of the impulsive fluid force that a breaking water wave might exert on the internal surfaces of a narrow crack, or crevice, in a sea wall. The crack might be the gap between two blocks in a blockwork structure, or the space opened up from a fracture in the masonry or natural rock. This enables estimates to be made of the stresses acting in the wall; these stresses could cause the constituent blocks of a breakwater, or other coastal structure, to move.

Bagnold (1939) was the first to show that at a fixed point on a vertical wall the pressure, during impact, initially rises to a peak value, p_{pk}, and then decreases. The increase and decrease together last for a time Δt, which is normally from one to 10 ms. This study focuses on a wave impact, which at full scale might exert a pressure of several atmospheres over this brief time interval.

Hattori (1994) and Chan and Melville (1988) report a wide scatter in both p_{pk} and Δt at laboratory scales. In a plot of field data, Bullock et al. (2000) in their Fig. 8 show that for any fixed Δt, p_{pk} may have a definite maximum. Also, the highest values of p_{pk} are associated with the smallest values of Δt. Bagnold (1939) suggested that the product $p_{\mathrm{pk}}\Delta t$ is a more consistent measure of impact among the scattered data. This led him to consider the time-integral of the pressure, a quantity referred to in this paper as the pressure impulse, P. More recent measurements by Allsop et al. (1996) also demonstrate the consistency of P.

* Corresponding author. Present address: Department of Physics, Trinity College, Dublin 2, Ireland. Fax: +353-1-671-1759.

E-mail addresses: coxs@tcd.ie (S.J. Cox), m.cooker@uea.ac.uk (M.J. Cooker).

0378-3839/01/$ - see front matter
PII: S0378-3839(00)00062-4

The definition of pressure impulse used here is

$$P(x,y,z) = \int_{t_b}^{t_a} p(x,y,z,t)\,\mathrm{d}t \tag{1}$$

where t_b and t_a are the times at the beginning and end of the pressure pulse or spike, x, y, z are Cartesian coordinates of position and p is the pressure (above atmospheric datum). The pressure impulse idea removes time from the equations of motion, but p_{pk} can be estimated from a calculated value of P using the approximate relation

$$P \approx \frac{1}{2} p_{pk} \Delta t. \tag{2}$$

That is

$$p_{pk} \approx \frac{2P}{\Delta t}. \tag{3}$$

However, since Δt is prone to uncertainty, any estimate of p_{pk} is also uncertain. Therefore, in the present work, a case is presented where the pressure impulse can by itself give useful information about the violent effects of wave impact.

For extreme impacts p_{pk} may be very large and Δt very small, but the product given in Eq. (2) will remain finite. The integral of P over a plane surface is the impulse which the impacting fluid exerts on that surface.

These ideas, which have been explained by Cooker and Peregrine (1990, 1995) and Chan (1994) for wave impacts, are now applied to the impulsive flow in a crack. For a crack which initially contains both air and water, the problem is complicated by (i) the possibility of fluid impacting the interior surfaces, and (ii) the reaction of air pockets and air bubbles to applied pressure.

Müller (1997) has instigated an experimental study into pressure propagation into cracks in sea walls. He measured the impact pressures on a vertical wall and then in a vertical crack in the wall. The top of the crack was at still water level so that it remained saturated with fluid throughout the experiments. Müller found that impact pressures on the wall propagated into the crack and were higher at the back of the crack. (If the crack was open to the atmosphere at the back, then the pressures were reduced on the rear transducer and were less than those on the front transducer.) The recorded pressures were, in general, only slightly less than those on the wall. He suggests that these are due to compression waves in the crack fluid, and that the impact pressures in these thin cracks cause large lateral pressures, which can exert high splitting stresses on the surrounding walls.

In this work the crack again remains saturated with water in order to simplify the analysis as much as possible. For the moment, any fluid compressibility will be due primarily to the presence of, perhaps microscopic, bubbles. It is possible to show that compressibility has a relatively minor effect on the pressure impulse. Relative to an incompressible fluid model the presence of compressibility reduces the predictions of peak pressure, as found by Peregrine and Thais (1996).

Another way to quantify compressibility is to take a relationship between density ρ and pressure p in the form

$$\rho(p) = \rho_0 + \frac{p}{c^2} \tag{4}$$

where ρ_0 is the equilibrium density of the fluid and c is the constant speed of sound in the medium. Müller (1997) has measured c to be as low as 50 m/s for pulses travelling in a laboratory crack under fluid-saturated conditions. Now consider Euler's equations:

$$\frac{\partial \underline{u}}{\partial t} + (\underline{u}\cdot\nabla)\underline{u} = -\frac{1}{\rho}\nabla p - g\underline{k} \tag{5}$$

where $\underline{u}$ is the velocity, g is the acceleration due to gravity, $\underline{k}$ is a unit vector pointing vertically up and ∇ is the gradient operator $(\partial/\partial x, \partial/\partial y, \partial/\partial z)$. Substitution of (4) and expansion in a power series gives

$$\frac{\partial \underline{u}}{\partial t} + (\underline{u}\cdot\nabla)\underline{u} = -\frac{\nabla p}{\rho_0}\left(1 - \frac{p}{\rho_0 c^2} + \dots\right) - g\underline{k}. \tag{6}$$

Even if a high value of $p = 6\times10^5$ N/m^2 is taken, and a rather low value of $c = 50$ m/s, the dimensionless factor in Eq. (6) is $p/\rho_0 c^2 \approx 0.24$, which is small compared with one. So Eq. (6) is well-approximated by its limiting form $c\to\infty$ for incompressible fluid:

$$\frac{\partial \underline{u}}{\partial t} + (\underline{u}\cdot\nabla)\underline{u} = -\frac{1}{\rho_0}\nabla p - g\underline{k} \tag{7}$$

with which the analysis begins in Section 2.

The definition of P in Eq. (1) remains valid for a compressible fluid because one can adjust the time limits t_b and t_a to be the instants just before and just after the arrival of a wave-impact pressure pulse. The further away one is from the point of impact, the later the times t_b and t_a must be chosen. The computation of P can be performed in the same way as for an incompressible fluid, as explained in this paper, but due care must be taken in estimating the associated peak pressure and the time of its occurrence.

By treating an incompressible fluid the model is incapable of accounting for the energy losses from compression waves propagating into cracks, reported by Müller et al. (2000). However, the most recent measurements (Müller and Makarov, personal communication) indicate that the pressure impulse varies by only $\pm 10\%$ among measurements made at four positions along the length of a 60-cm-long closed crack. For the same data, the peak pressure halves during the propagation of the pressure pulse over the same distance.

Future theoretical work with a compressible fluid may be able to account for dissipative effects, finite sound speed and the complex response of bubbles to violent impacts. The model of incompressible flows presented here gives the engineer useful information as to the most extreme conditions likely to occur. The model requires as input data the pressure impulse at the seaward edge; this information can be obtained from the theoretical wave impact work of Cooker and Peregrine (1990, 1995) and Chan (1994), who show that P is directly proportional to the speed of impact, wave height and fluid density. The model allows us to calculate $P(x,y)$ inside a crack whose median surface is described by Cartesian coordinates (x,y). From P one can calculate the sudden change in the fluid velocity inside the crack which is brought about by the impact. The model also quantifies the total impulse I on the internal faces of the crack. This impulse is directed normal to the plane of the crack and it is suggested that the impulse is responsible for moving blockwork. Depending on the orientation of the crack, the impulse can either lift a block or push it parallel to the line of the sea wall or even impel the block seawards. Expressions for I turn out to be quite simple for a plane crack (which is open only on its seaward edge): I is directly proportional to the area of the interior surface of the crack.

The rest of the paper is arranged as follows: the equations of pressure impulse theory are derived in Section 2 and the discussion in Section 3 motivates the application of the general theory to pressure impulses in a crack. In Section 4 the partial differential equation for $P(x,y)$ is derived for a crack whose height (i.e. smallest dimension) $h(x,y)$ varies with position. This is solved for the simple case where both P and h depend on x alone in Section 5.1. Solutions for P which depend upon both x and y are summarised in Section 5.2 and are derived in Appendix A. The effect on a solid block due to an uplifting or a laterally directed impulse are discussed in Section 6. Under the restoring forces of weight and friction the displacement of a block can be estimated.

2. Pressure impulse theory

Over the duration of the impact, the velocity field before impact, $\underline{u}_b$, is regarded as quite distinct from the velocity field after impact, $\underline{u}_a$. While before and after impact the velocity may vary in time, suppose that there is a short time interval $[t_b,t_a]$ during which the acceleration of the fluid, $\partial\underline{u}/\partial t$, greatly exceeds its value at all other times. This causes a rapid rise and fall in the pressure throughout the fluid and has striking consequences for the equations of motion.

Integrating Euler's equation (Eq. (5)) with respect to time over the short duration of the impact, $\Delta t = t_a - t_b$, gives

$$\underline{u}_a - \underline{u}_b + \int_{t_b}^{t_a} (\underline{u}\cdot\nabla)\underline{u}\,\mathrm{d}t = -\frac{1}{\rho}\nabla\int_{t_b}^{t_a} p\,\mathrm{d}t - g\Delta t\underline{k} \tag{8}$$

(where the subscript from the constant fluid density has been dropped). Introduction of a length scale L and a velocity scale u_0 shows that (away from the free surface where a jet of high velocity may be formed) the second term is of order $\Delta t u_0^2/L$ and the last term is of order $g\Delta t$. These are both small compared with $|\underline{u}_a - \underline{u}_b|$, which is of order u_0. The

only remaining term to balance Eq. (8) is the pressure integral. This gives, approximately, that

$$\underline{u}_a - \underline{u}_b = -\frac{1}{\rho}\nabla P \tag{9}$$

where P is the pressure impulse defined in Eq. (1).

If the fluid is incompressible before impact and after impact, $\nabla \cdot \underline{u}_b = 0$ and $\nabla \cdot \underline{u}_a = 0$, then the divergence of Eq. (9) shows that

$$\nabla^2 P = P_{xx} + P_{yy} + P_{zz} = 0 \tag{10}$$

where subscripts denote partial derivatives. Therefore, P satisfies Laplace's equation throughout the fluid. Eq. (10) is independent of time, and can be solved in the domain occupied by the fluid at the start of the impact. Appropriate Neumann or Dirichlet boundary conditions can be supplied to solve for P, which as well as giving information on peak pressures, will determine the velocity field after impact through Eq. (9), in which $\underline{u}_b$ is prescribed and needed in order to fix the boundary conditions for P. It is assumed that the walls of the crack are impermeable so that equating the normal derivative of P to zero will be the relevant boundary condition, corresponding to $\underline{u}_a = \underline{u}_b = 0$ in Eq. (9). Notice also that the curl of Eq. (9) shows that the vorticity is the same before and after impact, so the flow need not be irrotational.

Cooker and Peregrine (1995) calculate the pressure impulse in a fluid domain, D, whose shape models a sea wave at its moment of impact against a vertical wall of height H. D is the region $x \geq 0$, $-H \leq y \leq 0$, with the wall at $x = 0$ and the horizontal sea bed at $y = -H$. Boundary conditions of $P = 0$ are prescribed on the free surface $y = 0$, $P \to 0$ as $x \to \infty$ and $\partial P/\partial y = 0$ on the sea floor. The boundary condition on the wall is $\partial P/\partial x = -\rho u_0$ where the wave impacts and $\partial P/\partial x = 0$ below this impact zone. The resulting distribution of P is shown in Fig. 1, for an example where the wave breaks over the top half of the wall. The wavefront hits the wall in the negative x direction (i.e. it moves from right to left before impact) with constant horizontal velocity component, $-u_0$. The crack is assumed to be beneath the impact zone (i.e. in the lower half of the wall) so that before impact the fluid in the crack is at rest ($\underline{u}_b = 0$).

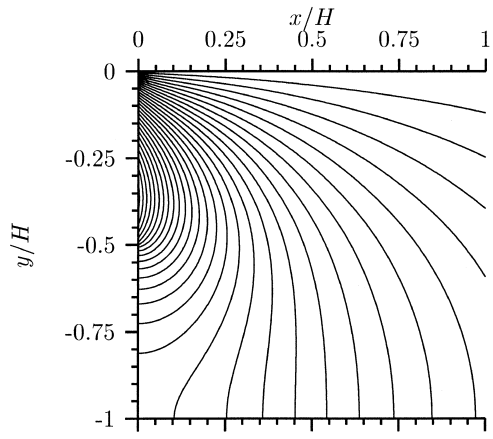

Fig. 1. Lines of constant pressure impulse for a wave impacting with velocity u_0 on the top half of the wall, $x = 0$, $y \in [-0.5H, 0]$, with a vertical front face. Contour separation is $0.01\ \rho u_0 H$ and $P = 0$ on the free surface $y = 0$.

The contours in Fig. 1 reveal a large gradient of pressure impulse acting down the lower part of the wall. This gradient is directly proportional to the finite change in flow velocity which occurs throughout the fluid domain during the impact, so that where the contours are close together there is a high-speed flow after impact, directed normal to the contours. Thus, at the origin a high-speed vertical jet is expected.

3. Crack geometry and boundary conditions

In a sea wall there are cracks through which water can flow, and the interconnection of individual cracks permits hydrodynamic pressures to be transmitted deep into the wall. The purpose of this section is to describe, with the aid of Fig. 2, the geometry of a crack (or crack network) in a sea wall, how the small width of the crack simplifies the fluid flow equation and what boundary flow conditions can be applied.

A typical crack contains a stratum of fluid that is thin. That is, the distance h between the crack walls is much less than the depth or width of the crack. To a good approximation, the fluid flows parallel to the walls, and more quickly where h is smaller (see Lamb, 1932, Art. 80). In the present problem, the fluid in the crack is driven by gradients in the

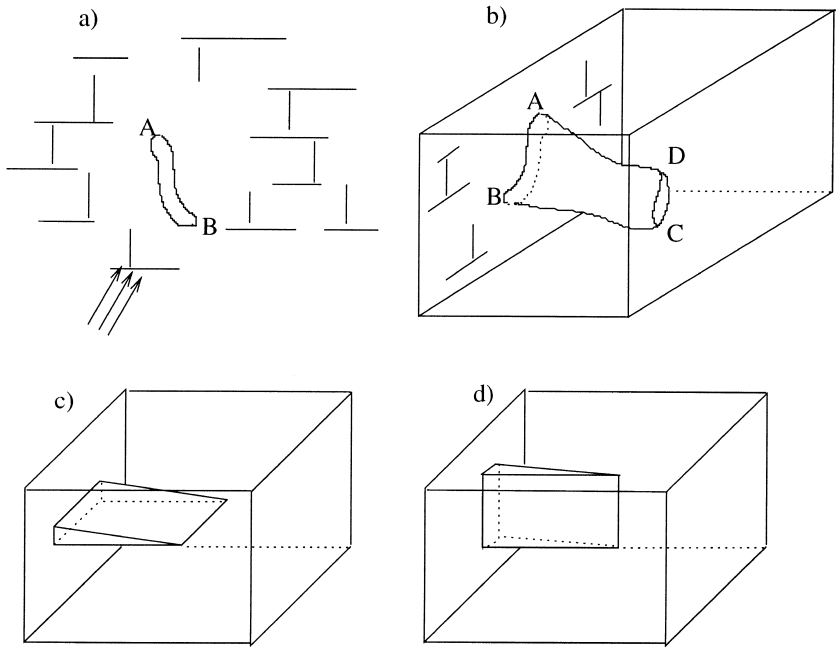

Fig. 2. The crack geometry. (a) Waves approach, in the direction shown by the arrows, towards the face of the sea wall in which there is a crack AB. (b) This view of the back of the wall shows how the same crack extends backwards from AB, to become the crack with area ABCD. Since the crack is thin and the pressures exerted are much greater than hydrostatic, the fluid flow in this curved stratum can be approximated by flow in (c) a horizontal crack or (d) a vertical crack, where the side walls are now plane (or nearly plane).

pressure impulse, which varies with position according to changes in h. Since the crack is thin, much can be inferred about results in curved cracks (as in Fig. 2b) from results for cracks which have one wall plane and the other nearly plane (Fig. 2c and d).

The pressure exerted in the crack is many times greater than any hydrostatic pressure due to the weight of the fluid alone. Therefore the orientation of the crack has little direct effect on the pressure impulse distribution, and the governing equation treats the horizontal and vertical cracks in Fig. 2c and d as the same.

Inside the wall the edges of a single crack are treated as impermeable, but where two cracks join along a common edge the pressure impulse, P, and the quantity $\partial P/\partial x$ are continuous across the junction. (Here x is a coordinate that crosses the join perpendicular to the common edge.) It is assumed that the crack walls are rigid; this is reasonable in the early stages of damage when cracks are still thin and the surrounding blocks are as yet unmoved. On the seaward edge, P is given from a previous calculation. Different data would be used in the cases illustrated in Fig. 2c and d: in (c) a uniform value of P may be appropriate, but (d) requires that P vary with height up the wall. In this case Fig. 1 suggests the validity of a linear approximation in a small interval below the impact zone, $y \approx -0.65H$, of $P \approx 0.5(1 + y/H)(\rho u_0 H)$. It is assumed that P in the exterior calculation is changed little by the presence of the cracks in the wall, which is reasonable if there is no appreciable net flux from the wave into the crack, such as might occur in a fluid saturated crack. For a closed crack (in which h shrinks to zero and hence the walls meet) $\partial P/\partial x = 0$ must be prescribed at the closed end. However, if the back of the crack is open to the air (with $p = 0$) then $P = 0$ must be prescribed as the free surface boundary condition. This condition is also appropriate for the back of an open crack which lies submerged a distance d, in still water. In this case $p = \rho g d$ and $P = \rho g d \Delta t$ which is negligible (for the short times of impact which we treat) compared with the pressure impulse values we expect at the entrance of the

crack. Therefore, $P = 0$ is again an appropriate free-surface boundary condition.

The main purpose for calculating P is to find the net impulse $\underline{I}$ on the crack walls, which is determined by integrating $P\hat{\underline{n}}$ over one wall, where $\hat{\underline{n}}$ is the unit normal to the wall's surface. The impulse can be interpreted as the product of a force $\underline{F}$ of large modulus and a short time Δt, so $\underline{F} = \underline{I}/\Delta t$. This impulsive force, $\underline{F}$, on the roof of the crack can be compared with, for example, the forces of block restraint and weight. Further, once P has been calculated, the velocity field in the crack can be found via Eq. (9), so that information will be available on how loose material in the crack will be moved around.

The analysis of the crack interior begins by assuming that the crack is thin, so that the pressure impulse changes little over the height of the crack. Then a two-dimensional equation for the pressure impulse in a three-dimensional crack can be derived. This is solved for several different geometries: the sides of blocks are often plane surfaces placed face-to-face and joined by cement. If the cement has eroded away then a crack with plane walls remains. A network of such cracks between many blocks thus might consist of thin plane strata, each connected to its neighbours along edges. Therefore, a crack is modelled which is composed of plane surfaces, which give the crack a height that varies with position. This distance between the crack walls is necessarily everywhere much less than the length or width of the plane surfaces which compose each of the crack's sidewalls. If the pressure impulse at the seaward end of a simple crack, where h depends only upon the distance x away from the seaward end, is constant ($P = P_0$), then because the walls are impermeable, the pressure impulse is the same constant, P_0, throughout the crack. If this crack is plane-sided, with unit normal $\hat{\underline{n}}$ to the plane, and if the crack area is A (ABCD in Fig. 2b), then $\underline{I} = P_0 A\hat{\underline{n}}$. Thus, the broader and deeper the crack the greater the impulse. However, if the crack is uniform in height and open to the atmosphere at the back ($P = 0$), then the solution for P decreases linearly from the front of the crack to the back, $P = P_0(1 - x/L)$, where L is the length of the crack and $x \in [0, L]$ is a coordinate along the base of the crack. Note that x could also be the arc length along the base of some more complicated crack, in which case P would be the same, provided that the crack was still uniform in height. P is found in some more complicated cracks in Section 5. The discussion in Section 6 is concerned with the effect of the wave impact on a crack beneath a large concrete block, such as might be found in a sea wall. The conclusions are summarised in Section 7.

4. An equation for the pressure impulse in a crack

Consider two almost parallel, impermeable, surfaces, S_1 and S_2, the gap between which is filled with fluid, as in Fig. 3. In the fluid domain, P satisfies the three-dimensional Laplace's equation

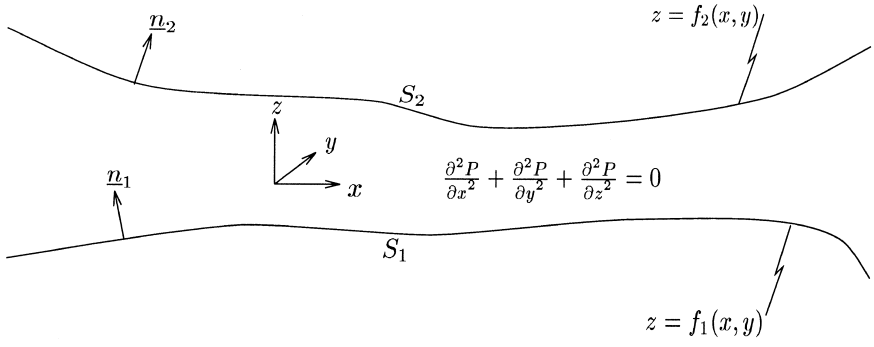

Fig. 3. Notation for calculating the pressure impulse in a crack. S_1 and S_2 are impermeable surfaces confining incompressible fluid and $\underline{n}_1$ and $\underline{n}_2$ are the respective normals. S_1 is given by $z = f_1(x,y)$ and S_2 by $z = f_2(x,y)$. The pressure impulse, P, satisfies the three-dimensional Laplace's equation with zero normal derivative on the bounding surfaces.

(Eq. (10)), $\nabla^2 P = 0$. The boundary conditions are that the walls are impermeable:

$$\nabla P \cdot \underline{n}_i|_{S_i} = 0, \quad i = 1, 2 \tag{11}$$

where $\underline{n}_i$ is the normal to the surface S_i. If S_i is defined by the equation $z = f_i(x, y)$ then $\underline{n}_i = (-\partial f_i/\partial x, -\partial f_i/\partial y, 1)$ and Eq. (11) becomes

$$\left.\frac{\partial P}{\partial z}\right|_{S_i} = \left.\frac{\partial P}{\partial x}\right|_{S_i} \frac{\partial f_i}{\partial x} + \left.\frac{\partial P}{\partial y}\right|_{S_i} \frac{\partial f_i}{\partial y}, \quad i = 1, 2. \tag{12}$$

Integrating Laplace's equation across the height of the crack, from $z = f_1$ to $z = f_2$, for fixed x and y gives (where x, y and z subscripts denote derivatives)

$$\int_{f_1}^{f_2} P_{xx} + P_{yy} + P_{zz}\,\mathrm{d}z = \int_{f_1}^{f_2} P_{zz}\,\mathrm{d}z + \int_{f_1}^{f_2} P_{yy}\,\mathrm{d}z + P_z|_{S_2} - P_z|_{S_1} = 0. \tag{13}$$

If S_i deviates little from the (x, y)-plane then both of the derivatives of each of the f_i are small: f_{1x}, f_{1y}, f_{2x}, $f_{2y} \ll 1$. Thus, Eq. (12) implies that $\partial P/\partial z$ is small compared with $\partial P/\partial x$ and $\partial P/\partial y$ on each of the bounding surfaces. Therefore, P varies little across the gap, and consequently the x and y derivatives of P vary little across the gap, and can be treated as independent of z. Thus, Eq. (13) becomes, approximately,

$$P_{xx}(f_2 - f_1) + P_{yy}(f_2 - f_1) + P_x \frac{\partial f_2}{\partial x} + P_y \frac{\partial f_2}{\partial y} - P_x \frac{\partial f_1}{\partial x} - P_y \frac{\partial f_1}{\partial y} = 0. \tag{14}$$

Defining $h(x, y) = f_2 - f_1$ (and neglecting terms of order h^3) gives

$$hP_{xx} + hP_{yy} + h_x P_x + h_y P_y = \nabla \cdot (h \nabla P) = 0 \tag{15}$$

where ∇ is now the two-dimensional gradient operator. Eq. (15) reduces to a two-dimensional Laplace's equation when h is constant, and in general, when either P or $\partial P/\partial n$ is specified on the boundary, the solution of Eq. (15) enables the pressure impulse in the crack to be found, so it can be used to find the impulse on the roof of the crack.

In Section 5 the special type of problem where P depends on x alone is solved; two-dimensional solutions of Eq. (15) are discussed in Section 5.2.

5. Results

5.1. One-dimensional solutions in open cracks

Consider initially a crack where $h = h(x)$ and $P = P(x)$, such as might arise when the seaward boundary data for P is uniform along the crack opening. If the crack were closed at the back end then, since $\partial P/\partial n = 0$ on each of the bounding surfaces, the pressure impulse is constant and equal to the pressure impulse specified at the open boundary. Now consider a crack of length L, which is open at the back ($x = L$). As shown in Fig. 4, the boundary conditions are that P is specified at each end of the crack: $P(x = 0) = P_0 > 0$ and $P(x = L) = 0$. If it is assumed that the base of the crack is flat ($f_1 \equiv 0$), then $h(x) = f_2(x)$. Eq. (15) becomes

$$\frac{\mathrm{d}}{\mathrm{d}x}\left(h \frac{\mathrm{d}P}{\mathrm{d}x}\right) = 0, \tag{16}$$

since P is a function of x only, with solution

$$P(x) = P_0\left(1 - \int_0^x \frac{\mathrm{d}x'}{h(x')} \Big/ \int_0^L \frac{\mathrm{d}x'}{h(x')}\right). \tag{17}$$

Therefore, P decreases monotonically from the entrance to the back of the crack, and the gradient of pressure impulse, and hence the change in fluid speed, is highest where h is smallest. The impulse on the roof of the crack is

$$I = P_0\left(L - \int_0^L \int_0^x \frac{\mathrm{d}x'}{h(x')}\,\mathrm{d}x \Big/ \int_0^L \frac{\mathrm{d}x'}{h(x')}\right) \tag{18}$$

so that $I < P_0 L$.

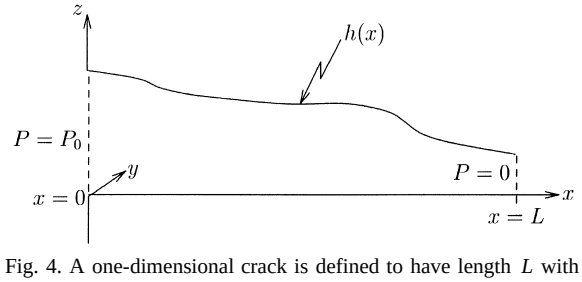

Fig. 4. A one-dimensional crack is defined to have length L with a flat base and a roof given by $z = h(x)$. The y-axis is normal to the plane of the figure and the boundary conditions are that $P(x = 0) = P_0$ and $P(x = L) = 0$.

Now $h(x)$ can be any function for which $1/h$ is integrable and $\mathrm{d}h/\mathrm{d}x$ is small. For example, if $h(x) = \alpha - \beta x$, where $\alpha > 0$ and $\alpha - \beta L > 0$, then

$$P(x) = P_0\left(1 - \frac{\log(1-\beta x/\alpha)}{\log(1-\beta L/\alpha)}\right). \tag{19}$$

If $\beta > 0$ the greatest change in fluid speed occurs at the back of the crack, but if $\beta < 0$ then this occurs at the seaward end, where the crack is thinner. From Eq. (18), the impulse on the roof of this crack is

$$I = P_0\left(\frac{L}{\log(1-\beta L/\alpha)} + \frac{\alpha}{\beta}\right) \tag{20}$$

per unit length of crack normal to Fig. 4. Notice that as $\beta \to 0$, Eq. (19) gives the solution for a crack of constant height, $P(x) = P_0(1 - x/L)$. In this case, the pressure impulse varies linearly between the two ends of the crack and the impulse on the roof of the crack is $I = (1/2)P_0 L$.

If the back of the crack is closed then $\alpha = \beta L$ (i.e. $h(L) = 0$) and the appropriate boundary condition is that $\mathrm{d}P/\mathrm{d}x = 0$ at $x = L$. Then in place of Eq. (19) the pressure impulse is given by $P(x) = P_0$ for all x, which is independent of the shape or height of the crack and is thus of especial interest for the study of realistic sea wall cracks. The impulse on the roof of the crack is $I = P_0 L$, which is greater than if the crack were open at the back end. Further, this impulse acts in the direction which widens the distance between the crack walls, if the walls are mobile.

It is also possible to find the pressure impulse in a crack with a roof which is defined as a continuous collection of segments for which P can be found from Eq. (17). To construct a solution, the general solution for P is found for each part of the roof and then P and $\mathrm{d}P/\mathrm{d}x$ are matched across the joins, to find the pressure impulses at the ends of each segment. This is demonstrated for the analysis of Section 5.2, where it is shown how to find P in a crack which is closed at one end, whose roof is made up of a continuous collection of piecewise linear segments and where P also varies in the y direction.

5.2. Two-dimensional solutions in piecewise linear closed cracks

The theory of Section 4 can also be applied to cracks in which $h = h(x)$ but the boundary condition at $x = 0$ varies with y, the axis normal to the plane of Fig. 4. The formulae satisfied by the pressure impulse in these cracks are derived in Appendix A, and two examples are given showing in detail how the field equation is solved, and how the pressure impulse distribution in the crack is affected by differences in the height of the crack, even though the fluid impulse on the roof of each crack is identical. The main conclusion is that, as for closed one-dimensional cracks, the impulse on the roof of the crack is proportional to both the area of the base of the crack and the mean pressure impulse at the seaward end of the crack. The calculation also gives information about how any loose material will be moved around the crack.

6. Discussion

When a wave breaks against a sea wall which contains a plane saturated crack, there is a distribution of pressure (impulse) across the plane of the crack. If the mean pressure impulse at the seaward end of the crack is P_0, if the crack is closed at the back, and if the area of one internal face of the crack is A then each face of the crack receives an impulse $\underline{I} = P_0 A\underline{\hat{n}}$, where $\underline{\hat{n}}$ is a unit normal to the plane of the crack, directed into the solid. This corresponds to an impulsive force of $\underline{F} = P_0 A\underline{\hat{n}}/\Delta t$.

A breaking wave in water of total depth H may be expected to hit a vertical sea wall with speed $u_0 = \sqrt{gH}$. The associated peak pressure impulse is $P_0 = 0.175\rho u_0 H$ (from Fig. 1) and so

$$|\underline{F}| = 0.175\frac{\rho g^{\frac{1}{2}} H^{\frac{3}{2}} A}{\Delta t}. \tag{21}$$

Now, suppose that A is the area of the base of a cubic block of side L which is part of the wall. Then the force $|\underline{F}|$ due to the pressurised water in the crack should be compared with the weight of the cube, $|\underline{W}| = \rho_B g L^3$, where ρ_B is the density of the wall material. It can exceed $|\underline{W}|$ if one of Δt, L or ρ_B is small enough, or H large enough. Fixing $H = 10$ m, $\rho_B = 3\rho$ and $\Delta t = 0.04$ s shows that $|\underline{F}| > |\underline{W}|$ if L is less than about 15 m.

For larger pressure impulses, or smaller Δt and ρ_B, it is likely that the wave will be able to (momen-

tarily) lift blocks even larger than those of side 15 m. Given the uncertainty in Δt, the corresponding minimum size of block which will not be moved by impact remains equally uncertain. These large upward forces may be decreased by reducing the area of the crack, for instance by avoiding the use of materials that allow broad horizontal fissures to develop.

A similar calculation can be applied to a crack with any orientation. For a crack in a vertical plane the resultant forces are horizontal and such lateral forces are likely to be resisted by the whole length of wall, but not at a site adjacent to damage or at the end of a wall under construction. Consider a block of mass $m = \rho_B AB$, where B is its breadth perpendicular to the crack. The block lies on a horizontal surface and the coefficient of friction between them is μ. The impulse due to the fluid in the crack moves the block a distance d before it is brought to rest by friction, where

$$d = \frac{I^2}{2\mu g m^2} = \frac{P_0^2}{2\mu g \rho_B^2 B^2}. \qquad (22)$$

Note the dependence of the displacement on the square of the impulse (or mean pressure impulse at the seaward end of the crack), and also the fact that it does not depend on the area of the crack. If the movement is resisted by a greater length of wall then B increases and d is reduced. The values posited above, together with $\mu = 1/2$, give $d = 3.4/B^2$, which, for sea walls, is likely to be a few centimetres. However, during a storm, the cumulative effect of many wave impacts could cause considerable displacement. In the absence of experimental data with which to compare the work of this paper, it is suggested that Eq. (22) may be one route by which the theory can be checked, without recourse to measuring detailed pressures within a crack.

If a crack extends up behind a block then these calculations predict a seaward force, as well as the lift force, which may or may not exceed the wave impact force. When a wave impacts against a wall, the pressure impulse field has a significant gradient along the sea floor, away from the wall. An object on the sea floor will therefore experience a seaward force, which can be calculated given knowledge of the pressure impulse. Then Eq. (15) can be applied to find P in the small gap beneath the object (see Cox, 1998).

7. Summary

This paper has demonstrated how to find the pressure impulse in a thin crack by deriving an equation for the pressure impulse, Eq. (15):

$$\nabla \cdot (h \nabla P) = \frac{\partial}{\partial x}\left(h \frac{\partial P}{\partial x}\right) + \frac{\partial}{\partial y}\left(h \frac{\partial P}{\partial y}\right) = 0$$

with the boundary conditions that P is given at the crack openings and that the normal derivative of P is zero where the crack is closed. In particular, with a view to discovering what happens when a wave impacts against the face of a water-saturated crack in a sea wall, the pressure–impulse distribution can be found in a crack of constant width, W, and length, L, whose roof is piecewise linear. The total impulse on the roof of the crack is then $I = P_0 LW$, where P_0 is the mean pressure impulse at the open end of the crack, so the impulse does not depend on the distribution of pressure impulse. This applies to a crack, which is closed at the back, but, conversely, if the crack is open to the air at the back then the impulse is reduced, for which a general formula is given.

If the block, which forms the roof, is a cube whose side length is less than a certain size then the force of a wave breaking against the wall in which the crack is situated could be large enough to overcome the gravitational force acting downwards, and lift the block. Also, the wave forces in cracks could cause considerable lateral stresses on the constituents of a sea wall. Further, these forces apply no matter how thin the crack, and do not change with varying crack height.

Calculation of the pressure impulse allows the fluid velocity gradients to be found, showing how debris may be swept into and out of the crack.

Notation

A	area of the base of the crack
B	breadth of the sea wall perpendicular to crack

d	distance moved by block in sea wall
D	fluid domain in which P is calculated
f_1, f_2	functions defining crack height
$\underline{F}$	impulsive force in crack
$\underline{g}$	acceleration due to gravity
h, h_m	crack height
H	water depth
I	impulse
$\underline{i}$, $\underline{j}$, $\underline{k}$	unit vectors in x, y, z directions
L	crack length
m	mass of block in sea wall
$\underline{n}$, $\underline{n}_1$, $\underline{n}_2$	normals to crack walls
p	fluid pressure
p_{pk}	peak fluid pressure
P, P_m	pressure impulse
P_0	pressure impulse at seaward end of crack
S_1, S_2	crack sides
t	time
t_{a}	time of end of impact
t_{b}	time of beginning of impact
$\underline{u}$	fluid velocity
$\underline{u}_{\mathrm{a}}$	fluid velocity after impact
$\underline{u}_{\mathrm{b}}$	fluid velocity before impact
u_0	impact velocity
W	weight of block in sea wall
x, y, z	Cartesian coordinates
α, α_m, β, β_m	parameters defining linear crack heights
Δt	$t_{\mathrm{a}} - t_{\mathrm{b}}$
μ	coefficient of friction
ρ	fluid density
ρ_{B}	density of sea wall material

Acknowledgements

SJC acknowledges financial support from both the School of Mathematics at the University of East Anglia and the UK Engineering and Physical Sciences Research Council, award number 96000215. MJC thanks UK EPSRC for the Blockwork Coastal Structures Network through grant GR/M00893.

Appendix A. Piecewise linear closed cracks

The work of Section 5.1 is extended here by considering a crack with a cross-section as in Fig. 5 but where the boundary data at $x = 0$ depends on y. This also shows how the matching process works for crack networks. The crack is closed at the back, the floor is flat, and the roof is made up of piecewise linear segments as demonstrated in Fig. 5. To simplify the analysis, the crack is assumed to be uniform in the y direction and to lie between impermeable walls at $y = 0$ and $y = y_1 > 0$. So the boundary data at $x = 0$ can be given as a Fourier cosine series in y, implying that although $h = h(x)$ only, $P = P(x, y)$.

A.1. The pressure impulse field

The starting point is Eq. (15):

$$\nabla \cdot (h \nabla P) = 0 \qquad \text{(A.1)}$$

where $h = h(x) = f_2(x)$ is the height of the crack, $f_1 \equiv 0$ and $P = P(x, y)$ is the pressure impulse in the crack. Recall that this is only valid for small $\mathrm{d}h/\mathrm{d}x$.

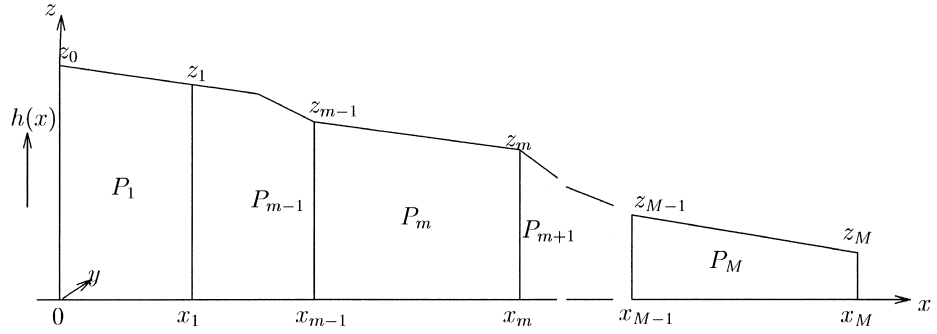

Fig. 5. A piecewise linear crack is divided into M sections, each of which is such that $h_m(x)$ is linear. The crack is uniform in the y direction (into the page), of length $L = x_M$, width $W = y_1$ and in the mth section $P = P_m(x, y)$.

The base of the crack is the plane $x \in [0, x_M]$, $y \in [0, y_1]$ and so the crack has a front-to-back length of $L = x_M$ and width $W = y_1$. The height, h, is a continuous collection of segments of the form $h_m(x) = \alpha_m - \beta_m x$, each defined on the interval $[x_{m-1}, x_m]$, where $\alpha_m \geq 0$, $x_0 = 0$ and $m = 1, \ldots, M$, as in Fig. 5. Then P is a differentiable function on each of the M segments and on the mth segment, $P = P_m(x, y)$, where each P_m satisfies Eq. (15).

The crack is closed at $x = x_M$ so that

$$\frac{\partial P_M}{\partial x}(x_M, y) = 0. \tag{A.2}$$

The flat sides $y = 0$ and $y = y_1$ are impermeable, so

$$\frac{\partial P_m}{\partial y}(x, 0) = \frac{\partial P_m}{\partial y}(x, y_1) = 0 \text{ for } m = 1, \ldots, M. \tag{A.3}$$

The open (seaward) end at $x = 0$ has specified data for P_1, given as a Fourier cosine series,

$$P_1(0, y) = P_0 + \sum_{j=1}^{\infty} S_j \cos(jy) \tag{A.4}$$

for some constant P_0. Notice that if the seaward condition is constant, $P_1(0, y) = P_0$, then the pressure impulse solution in the crack is P_0 everywhere. To satisfy Eq. (A.3), solutions for P_m must be of the form

$$P_m = P_0 + \sum_{n=1}^{\infty} f_{mn}(x) \cos\left(\frac{n\pi y}{y_1}\right)$$

$$\text{for } m = 1, \ldots, M. \tag{A.5}$$

So for each h_m the following equation must be solved:

$$\frac{\mathrm{d}^2 f_{mn}}{\mathrm{d}x^2} + \frac{h_m'}{h_m}\frac{\mathrm{d} f_{mn}}{\mathrm{d}x} - \left(\frac{n\pi}{y_1}\right)^2 f_{mn} = 0. \tag{A.6}$$

A.1.1. An arbitrary segment

For an arbitrary segment ($m \neq M$), there are two possibilities (given below).

• (i) h_m is a decreasing function of x (if h_m is increasing then the procedure is analogous),

$$h_m(x) = z_m + \left(\frac{x_m - x}{x_m - x_{m-1}}\right)(z_{m-1} - z_m) \tag{A.7}$$

and consequently it is convenient to define

$$\xi_m(x) = -\frac{h_m}{h_m'} = \frac{x_m z_{m-1} - x_{m-1} z_m}{z_{m-1} - z_m} - x \tag{A.8}$$

for $x \in [x_{m-1}, x_m]$. With this change of variable, Eq. (A.6) becomes

$$\frac{\mathrm{d}^2 f_{mn}}{\mathrm{d}\xi_m^2} + \frac{1}{\xi_m}\frac{\mathrm{d} f_{mn}}{\mathrm{d}\xi_m} - \left(\frac{n\pi}{y_1}\right)^2 f_{mn} = 0 \tag{A.9}$$

with solutions

$$f_{mn}(x) = A_{mn}\frac{I_0(n\pi\xi_m(x)/y_1)}{I_0(n\pi\xi_m(x_m)/y_1)} + B_{mn}\frac{K_0(n\pi\xi_m(x)/y_1)}{K_0(n\pi\xi_m(x_m)/y_1)} \tag{A.10}$$

where I_0 and K_0 are modified Bessel functions of order zero. Then

$$P_m(x, y) = P_0 + \sum_{n=1}^{\infty} \cos\left(\frac{n\pi y}{y_1}\right) \times \left[A_{mn}\frac{I_0(n\pi\xi_m(x)/y_1)}{I_0(n\pi\xi_m(x_m)/y_1)} + B_{mn}\frac{K_0(n\pi\xi_m(x)/y_1)}{K_0(n\pi\xi_m(x_m)/y_1)}\right]. \tag{A.11}$$

• (ii) h_m is constant,

$$h_m(x) = z_{m-1}, \tag{A.12}$$

and Eq. (A.6) becomes

$$\frac{\mathrm{d}^2 f_{mn}}{\mathrm{d}x^2} - \left(\frac{n\pi}{y_1}\right)^2 f_{mn} = 0 \tag{A.13}$$

with solutions

$$f_{mn}(x) = A_{mn}\frac{\cosh(n\pi x/y_1)}{\cosh(n\pi x_m/y_1)} + B_{mn}\frac{\sinh(n\pi x/y_1)}{\sinh(n\pi x_m/y_1)}. \tag{A.14}$$

Then

$$P_m(x, y) = P_0 + \sum_{n=1}^{\infty} \cos\left(\frac{n\pi y}{y_1}\right) \times \left[A_{mn}\frac{\cosh(n\pi x/y_1)}{\cosh(n\pi x_m/y_1)} + B_{mn}\frac{\sinh(n\pi x/y_1)}{\sinh(n\pi x_m/y_1)}\right]. \tag{A.15}$$

A.1.2. The closed segment

For the closed segment, $h = h_M$, (Eq. (A.2)), the zero-flux condition at $x = x_M$, is applied on a vertical wall. There are again two possibilities (given below).

• (i) h_M is a decreasing function of x, when Eq. (A.2) is applied to Eq. (A.11) at $x = x_M$ gives $B_{Mn} = 0$ and

$$P_M(x,y) = P_0 + \sum_{n=1}^{\infty} \cos\left(\frac{n\pi y}{y_1}\right) A_{Mn} \frac{I_0(n\pi\xi_M(x)/y_1)}{I_0(n\pi\xi_M(x_M)/y_1)} \tag{A.16}$$

A special case of this solution is when h_M decreases to zero at $x = x_M$. Then

$$h_M(x) = z_{M-1}\frac{x_M - x}{x_M - x_{M-1}} \tag{A.17}$$

and $\xi_M(x) = -h_M/h'_M = x_M - x$ so that instead of the more general Eq. (A.16) one obtains

$$P_M(x,y) = P_0 + \sum_{n=1}^{\infty} \cos\left(\frac{n\pi y}{y_1}\right) \times A_{Mn} I_0(n\pi(x_M - x)/y_1) \tag{A.18}$$

• (ii) h_M is constant. Then the solution for P_M is given by Eq. (A.15), and applying Eq. (A.2) gives

$$P_M(x,y) = P_0 + \sum_{n=1}^{\infty} A_{Mn}\cos\left(\frac{n\pi y}{y_1}\right) \times \frac{\cosh(n\pi(x_M - x)/y_1)}{\cosh^2(n\pi x_M/y_1)} \tag{A.19}$$

A.1.3. The complete solution

The solution for P is completed by applying Eq. (A.4) to P_1 at $x = x_0 = 0$ and by matching P_m and $\partial P_m/\partial x$ at each x_m, $m = 1,\ldots,M-1$; that is

$$P_m(x_m) = P_{m+1}(x_m),$$
$$\frac{\partial P_m}{\partial x}(x_m) = \frac{\partial P_{m+1}}{\partial x}(x_m) \quad \text{for } m = 1,\ldots,M-1. \tag{A.20}$$

This gives a system of $2M-1$ equations for each $n \geq 1$,

$$A_{1n}\,p(0) + B_{1n}\,s(0) = S_n$$
$$A_{mn} + B_{mn} = A_{(m+1)_n}\,p(m) + B_{(m+1)_n}s(m) \quad \text{for } m = 1,\ldots,M-1$$
$$A_{mn}\,\bar{p}(m) + B_{mn}\bar{s}(m) = A_{(m+1)_n}\bar{\bar{p}}(m) + B_{(m+1)_n}\bar{\bar{s}}(m) \quad \text{for } m = 1,\ldots,M-1. \tag{A.21}$$

In this system the unknowns A_{mn} and B_{mn} are sought, with the expressions for $p(m)$, $s(m),\ldots$ and B_{Mn} chosen according to the choice of h_m and h_M, respectively, as given in Table 1. When $M \geq 2$ the system (A.21) can be solved using, for example, the computer algebra package Maple (Vr3). Then, once all the A_{mn}, B_{mn} have been expressed in terms of the S_m, the pressure impulse values, P_m, can be found from Eqs. (A.11), (A.15), (A.18) and (A.19) as required.

A.2. The impulses on a piecewise linear closed crack

In attempting to find the net fluid impulse, $\underline{I}$, on each segment of the roof and the back of the crack,

Table 1
Values of the constants for the system (A.21) in each of the two cases, where $h_m(x)$ either decreases with x or is constant

	Case (i) h_m decreasing	Case (ii) h_m constant
$p(m)$	$\dfrac{I_0(n\pi\xi_{m+1}(x_m)/y_1)}{I_0(n\pi\xi_{m+1}(x_{m+1})/y_1)}$	$\dfrac{\cosh(n\pi x_m/y_1)}{\cosh(n\pi x_{m+1}/y_1)}$
$s(m)$	$\dfrac{K_0(n\pi\xi_{m+1}(x_m)/y_1)}{K_0(n\pi\xi_{m+1}(x_{m+1})/y_1)}$	$\dfrac{\sinh(n\pi x_m/y_1)}{\sinh(n\pi x_{m+1}/y_1)}$
$\bar{p}(m)$	$\dfrac{I_1(n\pi\xi_m(x_m)/y_1)}{I_0(n\pi\xi_m(x_m)/y_1)}$	$\tanh(n\pi xm/y_1)$
$\bar{s}(m)$	$-\dfrac{K_1(n\pi\xi_m(x_m)/y_1)}{K_0(n\pi\xi_m(x_m)/y_1)}$	$\coth(n\pi x_m/y_1)$
$\bar{\bar{p}}(m)$	$\dfrac{I_1(n\pi\xi_{m+1}(x_m)/y_1)}{I_0(n\pi\xi_{m+1}(x_{m+1})/y_1)}$	$\dfrac{\sinh(n\pi x_m/y_1)}{\cosh(n\pi x_{m+1}/y_1)}$
$\bar{\bar{s}}(m)$	$-\dfrac{K_1(n\pi\xi_{m+1}(x_m)/y_1)}{K_0(n\pi\xi_{m+1}(x_{m+1})/y_1)}$	$\dfrac{\cosh(n\pi x_m/y_1)}{\sinh(n\pi x_{m+1}/y_1)}$
B_{Mn}	0	$-\tanh^2(n\pi x_M/y_1)$

note that, due to the presence of the cosine terms in the solutions for P, the only contribution to $\underline{I}$ comes from the constant term, P_0. Unit vectors $\underline{i}$, $\underline{j}$ and $\underline{k}$ are defined in the x, y and z directions, respectively, then the horizontal component of impulse from the seaward face of the crack is $P_0 y_1 z_0 \underline{i}$. ($z_0$ is the height of the crack at the wall face.) The impulse on the mth segment of the horizontal floor is $-P_0 y_1 (x_m - x_{m-1})\underline{k}$. Resolving components horizontally and vertically gives the impulse on the roof of each of the m segments:

$$\underline{I}_m = P_0 y_1 \big((z_{m-1} - z_m)\underline{i} + (x_m - x_{m-1})\underline{k} \big). \tag{A.22}$$

If the crack has the roof of its Mth segment horizontal then the $\underline{i}$ component of $\underline{I}_M$ is $P_0 y_1 z_{m-1}$ and it acts on the back wall rather than the roof. Notice then that any other segment with a horizontal roof has no horizontal component of impulse acting on it.

The total impulse on the roof and back of the crack is

$$\underline{I} = \sum_{m=1}^{M} \underline{I}_m = P_0 y_1 \big(z_0 \underline{i} + L\underline{k} \big). \tag{A.23}$$

The following conclusions, which are independent of the distribution of height within the crack, can now be drawn. The horizontal impulse on the roof of a crack of length L, width W and height H (at the seaward end) is $P_0 WH$ and the vertical impulse is $P_0 LW$. The horizontal impulse will be small, since it is directly proportional to the height of the crack. The vertical impulse is P_0 multiplied by the area of the crack roof, and is independent of the crack height. So the important physical conclusion is that the principle component of fluid impulse is directed normal to the plane of the roof, and will act so as to open up the crack, no matter how narrow it is. Also, this component of impulse does not depend upon the distribution of pressure impulse at the seaward end of the crack, only it's mean value.

A.3. Example: plane-sided slot

Consider a crack with a flat horizontal roof from the back to where it meets the seaward face of the wall in which it is situated. The height of the crack is arbitrary, though small, and there is just a single segment, $m = M = 1$. So, the crack is a thin rectangular box. Then Eq. (A.19) is applicable:

$$P(x,y) = P_0 + \sum_{n=1}^{\infty} A_n \cos(n\pi y/y_1) \times \frac{\cosh\big(n\pi (x_1 - x)/y_1\big)}{\cosh^2 (n\pi x_1/y_1)}. \tag{A.24}$$

Consider the crack to be in a vertical plane, similar to the crack in which Müller (1997) measured the pressures due to a breaking wave. A dimensional seaward boundary condition of $P(0,\ y) = (1 + y)(0.5\rho u_0 H)$ is taken from the earlier calculation shown in Fig. 1, as discussed in Section 3. This applies to a wave which impacts upon the top half of the wall, above the crack, with a uniform velocity profile. As a Fourier cosine series, $P(0,\ y)$ can be written

$$P(0,y)/(0.5\rho u_0 H) = 1 + y = 1 + \frac{y_1}{2} - \frac{4y_1}{\pi^2} \sum_{j=0}^{\infty} \frac{\cos\big[(2j+1)\pi y/y_1\big]}{(2j+1)^2}. \tag{A.25}$$

Comparing coefficients gives $A_n/\cosh(n\pi x_1/y_1) = S_n$, where

$$S_{2n} = 0 \quad \text{and} \quad S_{2n+1} = -\frac{4y_1}{\pi 2} \frac{1}{(2n+1)^2}, \tag{A.26}$$

and $P_0 = (1 + (1/2)y_1)(0.5\rho u_0 H)$. Then

$$\frac{P(x,y)}{0.5\rho u_0 H} = 1 + \frac{y_1}{2} - \frac{4y_1}{\pi^2} \sum_{n=0}^{\infty} \frac{\cos\big[(2n+1)\pi y/y_1\big]}{(2n+1)^2} \times \frac{\cosh\big((2n+1)\pi (x_1 - x)/y_1\big)}{\cosh\big((2n+1)\pi x_1/y_1\big)}. \tag{A.27}$$

This pressure impulse solution is shown in Fig. 6. The impulsive change in velocity is given by Eq. (9),

$\underline{u}_a - \underline{u}_b = -\nabla P/\rho$. If the fluid is stationary before impact ($\underline{u}_b = 0$) then the contours in Fig. 6 are interpreted as lines normal to $\underline{u}_a$. Where the contours are close together the speed, $|\underline{u}_a|$, is larger, such as near (0,0) (where $P = 1(0.5\rho u_0 H)$, its lowest value) and (0,3) (where $P = 4(0.5\rho u_0 H)$, its highest value). At the back of the crack the contours are spaced further apart which implies a slower induced flow. So the boundary condition applied at the seaward end of the crack will, in this case, induce a flow into the crack near (0,3) and out of the crack near (0,0). Any small particles of debris are also impelled by the pressure impulse field, and they will therefore be swept around the inside of the crack. This might be one mechanism by which solid particles become lodged in, or extracted from, crevices.

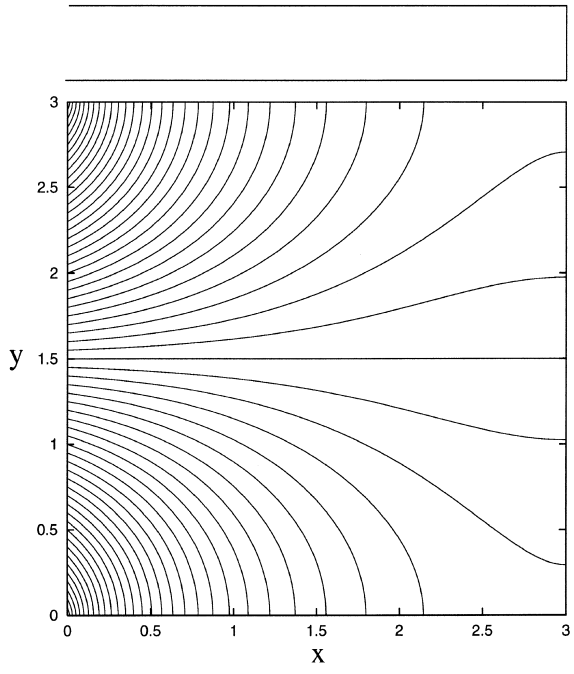

Fig. 6. The contours of constant pressure impulse for a rectangular crack with a flat horizontal roof, whose cross-section is shown in the upper part of the figure. The lower part of the figure is a plan view of the crack with contour separation $0.05(0.5\rho u_0 H)$ and $x_1 = 3.0$, $y_1 = 3.0$. The seaward boundary condition is $P(0,y) = (1+y)(0.5\rho u_0 H)$ and the contours are symmetric about the centreline of the crack, $y = 1.5$, (which follows from the cosine dependence) and show the variation of P away from P_0, the pressure impulse at the centre of the open end.

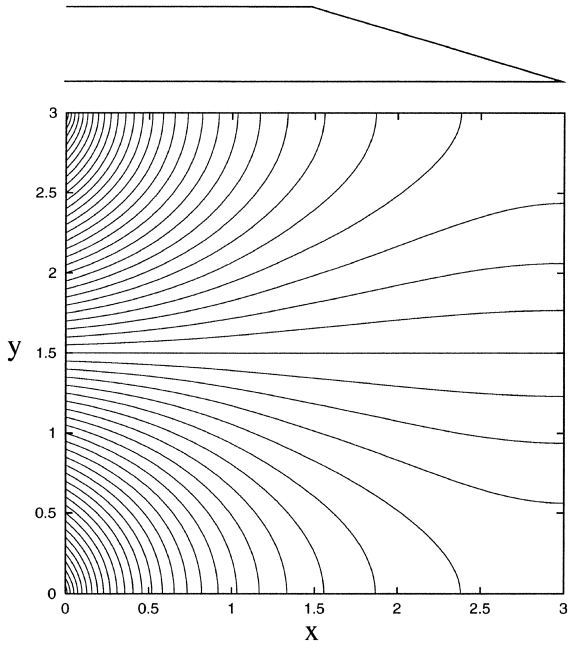

Fig. 7. The contours of constant pressure impulse, from Eqs. (A.31) and (A.32), for a chisel-shaped crack whose cross-section is shown in the upper part of the figure. These should be compared with those in Fig. 6. The seaward boundary condition is the same and the contour separation is again $0.05(0.5\rho u_0 H)$.

A.4. Example: Chisel-shaped slot

Now consider a crack with two sections: the seaward section ($m = 1$) has a horizontal roof and the other section ($m = 2$) has a sloping roof that joins the back edge to the seaward section. Thus

$$h_1 = \alpha_1 \text{ on } x \in [0, x_1] \text{ and}$$

$$h_2 = \alpha_1 \frac{x_2 - x}{x_2 - x_1} \text{ on } x \in [x_1, x_2], \tag{A.28}$$

which is illustrated at the top of Fig. 7. At the open end of the crack, Eq. (A.15) implies

$$P_1(x,y) = P_0 + \sum_{n=1}^{\infty} \cos\left(\frac{n\pi y}{y_1}\right) \times \left[A_{1n} \frac{\cosh(n\pi x/y_1)}{\cosh(n\pi x_1/y_1)} + B_{1n} \frac{\sinh(n\pi x/y_1)}{\sinh(n\pi x_1/y_1)} \right] \tag{A.29}$$

and at the sloping, back, end, Eq. (A.18) implies

$$P_2(x,y) = P_0 + \sum_{n=1}^{\infty} \cos\left(\frac{n\pi y}{y_1}\right) A_{2n} I_0\left(\frac{n\pi(x_2 - x)}{y_1}\right) \tag{A.30}$$

As in the previous example, the dimensional seaward boundary condition is $P(0,\ y) = (1+y)(0.5\rho u_0 H)$ so $P_0 = (1 + (1/2)y_1)(0.5\rho u_0 H)$. Applying the matching system from Eq. (A.21) requires the solution of

$$A_{1n} = S_n \cosh(n\pi x_1/y_1)$$

$$A_{1n} + B_{1n} = A_{2n} I_0(n\pi(x_2 - x_1)/y_1)$$

$$A_{1n}\tanh(n\pi x_1/y_1) + B_{1n}\coth(n\pi x_1/y_1) = A_{2n} I_1(n\pi(x_2 - x_1)/y_1)$$

where the S_n are given by Eq. (A.26). Then

$$A_{2n} = \frac{S_n}{I_0(n\pi(x_2 - x_1)/y_1)\cosh(n\pi x_1/y_1) - I_1(n\pi(x_2 - x_1)/y_1)\sinh(n\pi x_1/y_1)}$$

$$B_{1n} = S_n \cosh(n\pi x_1/y_1)\frac{I_1(n\pi(x_2 - x_1)/y_1) - I_0(n\pi(x_2 - x_1)/y_1)\tanh(n\pi x_1/y_1)}{I_0(n\pi(x_2 - x_1)/y_1)\coth(n\pi x_1/y_1) - I_1(n\pi(x_2 - x_1)/y_1)}$$

and

$$\frac{P_1(x,y)}{0.5\rho u_0 H} = 1 + \frac{y_1}{2} - \frac{4y_1}{\pi^2}\sum_{n=0}^{\infty}\frac{\cosh[(2n+1)\pi y/y_1]}{(2n+1)^2}\cosh[(2n+1)\pi x/y_1]\left[1 + \mathscr{I}_n^1\right] \tag{A.31}$$

$$\frac{P_2(x,y)}{0.5\rho u_0 H} = 1 + \frac{y_1}{2} - \frac{4y_1}{\pi^2}\sum_{n=0}^{\infty}\frac{\cosh[(2n+1)\pi y/y_1]}{(2n+1)^2}\mathscr{I}_n^2 \tag{A.32}$$

where

$$\mathscr{I}_n^1 = \tanh[(2n+1)\pi x/y_1]\frac{I_1(n\pi(x_2 - x_1)/y_1)\coth(n\pi x_1/y_1) - I_0(n\pi(x_2 - x_1)/y_1)}{I_0(n\pi(x_2 - x_1)/y_1)\coth(n\pi x_1/y_1) - I_1(n\pi(x_2 - x_1)/y_1)} \tag{A.33}$$

and

$$\mathscr{I}_n^2 = \frac{I_0((2n+1)\pi(x_2 - x)/y_1)}{I_0(n\pi(x_2 - x_1)/y_1)\cosh(n\pi x_1/y_1) - I_1(n\pi(x_2 - x_1)/y_1)\sinh(n\pi x_1/y_1)}. \tag{A.34}$$

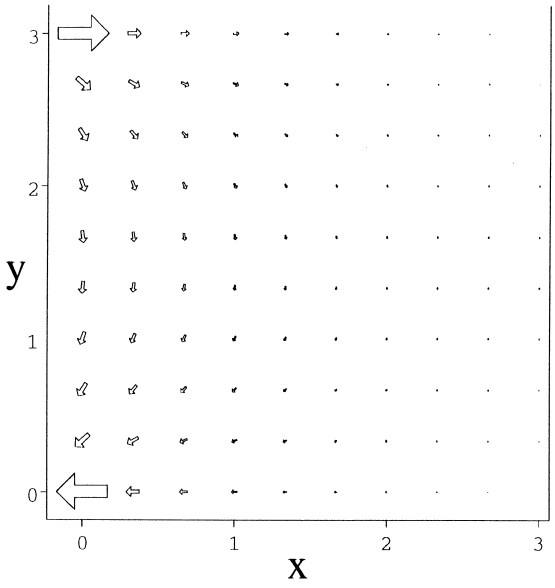

Fig. 8. The arrows show the direction and magnitude of the induced change in velocity of the fluid in the crack, $\underline{u}_a - \underline{u}_b$, as given by Eq. (9). The largest arrow corresponds to a speed of $2.1u_0$. It is evident that most of the motion occurs close to the seaward end of the crack.

The contours of constant P_1 and P_2 are plotted, in their consecutive domains, in Fig. 7. Comparing the contours with those in Fig. 6 shows that the effect of the sloping part of the roof is to increase the pressure impulse gradient along the back wall. Similar comments apply to those at the end of the previous example, except that the change in velocity will be higher along the back wall of this crack. Fig. 8 is a sketch of the velocity field for the flow induced by the seaward boundary condition given here, which is applicable to both examples.

References

Allsop, N.W.H., McKenna, J.E., Vicinanza, D., Whittaker, T.T.J., 1996. New design methods for wave impact loadings on vertical breakwaters and seawalls. Proc. 25th Intl. Conf. Coast. Eng., Orlando.

Bullock, G.N., Crawford, A.R., Hewson, P.J., Bird, P.A.D., 2000. Characteristics of wave impacts on a steep fronted breakwater. Proc. Coastal. Structures ’99, Santander.

Bagnold, R.A., 1939. Interim report on wave-pressure research. J. Inst. Civil Eng. 12, 201–226.

Chan, E.S., 1994. Mechanics of deep water plunging-wave impacts on vertical structures. Coastal Eng. 22, 115–133.

Chan, E.S., Melville, W.K., 1988. Deep-water plunging wave pressures on a vertical plane wall. Proc. R. Soc. Lond. A 417, 95–131.

Cooker, M.J., Peregrine, D.H., 1990. A model for breaking wave impact pressures. Proc. 22th Intl. Conf. Coast. Eng., Delft, The Netherlands.

Cooker, M.J., Peregrine, D.H., 1995. Pressure–impulse theory for liquid impact problems. J. Fluid Mech. 297, 193–214.

Cox, S.J., 1998. Pressure Impulses caused by Wave Impact. PhD thesis. School of Mathematics, University of East Anglia.

Hattori, M., 1994. Wave impact pressures on vertical walls and the resulting wall deflections. Proc. Intl. Workshop on Wave Barriers in Deepwaters, Yokosuka, Japan.

Lamb, H., 1932. Hydrodynamics. 6th edn. Cambridge Univ. Press, Cambridge.

Müller, G., 1997. Wave impact pressure propagation into cracks. Proc. Inst. Civil Eng Water Marit. Energy 124, 79–85.

Müller, G., Makarov, G., personal communication.

Müller, G., Allsop, N.W.H., Bruce, T., Cooker, M.J., Franco, L., 2000. Propagation of wave impact pressure into joints/cracks in blockwork breakwaters and seawalls. Proc. Coastal. Structures ’99, Santander.

Peregrine, D.H., Thais, L., 1996. The effect of entrained air in violent water wave impacts. J. Fluid Mech. 325, 377–397.